ANNALS OF GEOPHYSICS, 66, 6, SE635, 2023; doi:10.4401/ag-8964
OPEN ACCESS

On the relevance of the foreshocks in forecasting seismic mainshocks

Bogdan Felix Apostol*,[1] and Liviu Cristian Cune[2]

(1) National Institute for Earth Physics, Călugăreni Street, 12 Magurele, Ilfov, Romania
(2) National Institute of Physics and Nuclear Engineering, Magurele, Ilfov, Romania
MG-6, POBox MG-35, Romania

Article history: received March 3, 2023; accepted September 2, 2023

Abstract

We analyze the usefulness of the foreshocks in forecasting seismic mainshocks. The analysis is based on possible correlations which may exist between foreshocks and mainshocks. Such correlations are expressed by a previously established time-magnitude relationship, which indicates the presence of an abrupt magnitude-decreasing sequence of correlated foreshocks in the proximity of a mainshock. By fitting this formula, we are able to derive the occurrence time of a possible mainshock. Also, we can estimate the magnitude of the mainshock, providing we know the parameters of the background seismicity of the seismic region. We report here on the application of this procedure to three Vrancea (Romania) mainshocks, the l'Aquila (Italy), Yangbi (Yunnan, China) and Izmit (Turkey) earthquakes. The limitations of the procedure are discussed. Also, a discussion is included regarding the so-called temporal variability of the Gutenberg-Richter parameter in the proximity of a mainshock, as resulting from time-magnitude and time-time correlations.

Keywords: Time-magnitude correlations; Foreshocks; Mainshocks; Forecasting; Gutenberg-Richter parameter

1. Introduction

The prediction of the big earthquakes is a long standing problem in seismology [see, for instance, Stein and Wysession, 2003; Udias, 1999; and Jordan et al., 2011; van Stiphout et al., 2010; Gerstenberger et al., 2005]. It is well known that seismic mainshocks are accompanied by foreshocks and aftershocks, which are localized in the spatial and temporal relative proximity of the mainshocks. After a strong mainshock the focal region and its surroundings may be modified, and special, smaller aftershocks may appear [Omori, 1894; Utsu, 1965, Lippiello et al., 2015]. Similarly, the energy accumulated in the focal region may be released in advance by some, smaller foreshocks, which may announce the occurrence of a mainshock [Seif et al., 2019; Bouchon et al., 2013; Jones and Molnar, 1976, 1979]. It is reasonable to assume that such anomalous foreshocks and aftershocks, which may exhibit a certain connection with the mainshock, should have the hypocentres close to the focus of the mainshock and should occur in a restricted time window around the moment of the occurrence time of the mainshock. These accompanying seismic events, which are associated with the mainshock in space and time, may exhibit specific patterns in their space,

time, magnitude distributions. It seems reasonable to assume that such specific characteristics of the foreshocks might be useful in predicting the occurrence of the mainshocks. Obviously, such seismic events are correlated, in the sense that the characteristic parameters of an event depend on the characteristic parameters of the other. The correlations reflect a possible connection between the accompanying seismic events and the mainshock, as well as between themselves.

As important, and reasonable, as this problem may appear (called sometimes the "foreshock hypothesis", see, for instance, Petrillo and Lippiello, 2020; Mignan, 2014), it seems that specific procedures with a practical potential of application have not yet led to convincing results. The problem exhibits serious difficulties. Firstly, for instance, not all the foreshocks may be correlated to the mainshock; some of them may be regular, background, precursory earthquakes. Secondly, the sequence of correlated foreshocks may be interrupted by a sequence of regular earthquakes, or by so-called seismic gaps, possibly as a result of unknown local, structural changes in the focal region. Thirdly, correlated foreshocks may generate their own sequences of smaller, second-order (and higher-order) accompanying events, both in advance and after their occurrence, as it is well known from the epidemic-type aftershock sequence (ETAS) model [Saichev and Sornette, 2005; Helmstetter and Sornette, 2003; Ogata, 1988, 1998]. According to this model every seismic event in the sequence foreshocks-mainshock-aftershocks is correlated to every other seismic event in the sequence, and such correlations are hierarchical in their degree of magnitude.

The investigation of the problem was focused on the physical mechanism of occurrence of the foreshocks and the mainshocks, which is a difficult problem. On one hand, an astatic pre-slip over an extended area may lead to stress accumulation in the focus of the mainshock [Mignan, 2011; Bouchon et al., 2011; Ellsworth and Beroza, 1995; Ohnaka, 1992]. An intense seismic activity may occur, followed by a nucleation phase. Also, a random triggering of cascading earthquakes is possible, the mainshock included [Felzer et al., 2004; Helmstetter and Sornette, 2003; Ogata, 1988]. It was suggested that the mainshock preparation phase is controlled by the fault surface heterogeneities and the stress redistribution [Yamashita et al., 2021]. A critical analysis of these two competing models was done by Mignan [2014].

On the other hand, the well-known time variation of the Gutenberg-Richter parameter (β) for foreshocks (GR parameter), compared to aftershocks and the background seismicity (see, for example, Papazachos, 1975 and References therein), was recently documented by Gulia and Wiemer [2019] in some cases. The foreshock parameter β is lower than the background value (e.g., by 10%), while the aftershock parameter is higher than the background value (e.g., by 20%; see also Gulia et al., 2018, 2016 and References therein; De Santis et al., 2011). The variation of the parameter β in the foreshock sequence could be useful in forecasting mainshocks in some cases, though the analysis method employed by Gulia and Wiemer [2019] was questioned [Dascher-Cousineau et al., 2020, 2021; see also Gulia and Wiemer, 2021].

If existing, the forecasting potential of the foreshocks remains elusive as long as a quantitative description of the correlations is not available. Such a quantitative description should relate foreshocks characteristics to the time left until to the occurrence of the mainshock. We present in this paper such a quantitative relation between the magnitude M of the correlated foreshocks and the time τ until the occurrence of the mainshock, based on the time-magnitude correlations derived recently [Apostol, 2021]. We focus here on the main correlations which may connect the foreshocks (and the aftershocks) to the mainshock (and, of course, the mainshock to the foreshocks and the aftershocks). We show that such correlations, if present, may increase the Gutenberg-Richter parameter β for aftershocks, in agreement with some empirical observations. Also, we show that these correlations may be related to other type of correlations, called time-time correlations (or purely dynamical correlations [Apostol, 2021]). This connection affects the Gutenberg-Richter standard distribution in such a way that, if present, the parameter β decreases for foreshocks, in agreement with some other empirical observations. In general, the time-time correlations can be seen most conveniently in the roll-off effect present in the Gutenberg-Richter distribution at small magnitudes.

The time-magnitude relation between M and τ shows an abrupt decrease in magnitudes in the proximity of a mainshock (when τ tends to a small threshold time τ_0, see below). As such, the method is valid for a short-, and very short-, time forecasting (a circumstance which may question the practical utility of the method). From our tests, which we describe below, we may say that the practical procedure consists in monitoring continuously (daily, even hourly) the seismic activity in a focal region, prone to a mainshock. If a (relatively short) sequence of foreshocks can be fitted reasonably by the M-τ correlation law given here, we might be in the proximity of a mainshock. We can estimate the moment of the occurrence time of the mainshock, and, if we know the background seismicity parameters of the region, as described herein, we can even estimate the magnitude of the mainshock. It may happen

that the prediction fails, from various, unknown causes, as, for example, local structural changes intervening in the focal region (false positive). Also, not all magnitude-decreasing foreshock sequences are correlated foreshocks. We cannot say at this moment what is the degree of success of the method. This can only be estimated after a long series of tests, done in specific conditions. Also, it may happen that a mainshock occurs without being preceded by correlated foreshocks, such that we may have a false negative. However, there exist cases where the method may succeed, as shown below.

2. Background seismicity

As it is well known, the background seismic activity is governed by the Gutenberg-Richter (GR) statistical law. Its standard cumulative (exceedance) form is $P_{ex}(M) = e^{-\beta M}$, where $P_{ex}(M)$ is the probability of occurrence of an earthquake with magnitude greater than M and the GR parameter β varies in the range 1.15 to 3.45 (in decimal logarithms 0.5 to 1.5); the mean value $\beta = 2.3$ (in decimal logarithms $\beta = 1$) is usually accepted as a reference value [Stein and Wysession, 2003; Udias, 1999; Lay and Wallace, 1995; Frohich and Davis, 1993]. If the number of earthquakes with magnitude greater than M is $N(M)$, out of a total number N_0 of earthquakes in a given seismic region and a given long time interval T, we may write $P_{ex}(M) = N(M)/N_0 = N(M)t_0/T$, where t_0 is the inverse of a mean seismicity rate. The law is applied with a small-magnitude cutoff which accounts for the completeness magnitude of the catalog, or the well-known roll-off effect occurring at small magnitudes [Bhattacharya et al, 2009; Apostol, 2021; Pelletier, 2000]. Consequently, the parameter t_0 is a fitting parameter, like β. In its linear-logarithmic form the law reads

$$\ln[N(M)/T] = -\ln t_0 - \beta M \tag{1}$$

By fitting this law we can extract the parameters t_0 and β of the background seismicity. We performed such a fit for a set of 3640 earthquakes with magnitude $M \geq 3$ which occurred in Vrancea during 1981-2018. The resulting parameters are $-\ln t_0 = 11.32$ (t_0 measured in years) and $\beta = 2.26$ (with an estimated 15% error). We note that the value $\beta = 2.26$ is close to the reference value 2.3 given above. We use these data in the applications to Vrancea region, described below. The data for Vrancea have been taken from the Romanian Earthquake Catalog (2023), http://www.infp.ro/data/romplus.txt. A completeness magnitude $M = 2.2$ to $M = 2.8$ is usually accepted for Vrancea (a more conservative figure would be $M = 3$, [Enescu et al., 2008] and References therein), and the magnitude average error is $\Delta M = 0.1$. A similar fit, with slightly modified parameters, is valid for 8455 Vrancea earthquakes with magnitude $M \geq 2$ (period 1980-2019).

3. Foreshocks and aftershocks

Let us focus on the time-energy accumulation formula

$$t/t_0 = (E/E_0)^r \tag{2}$$

given in the Appendix A (equation (A4)).

Let us assume that at the moment t_1 a mainshock with energy E_1 and magnitude M_0 occurs. Further, we assume that a small energy E is released after a small lapse of time τ, as if the accumulation process continues and the mainshock would share a small amount of energy with an aftershock. Also, we may assume that a small amount of energy E is accumulated in excess at time τ before the mainshock, possibly by a local, structural change in the focal region, and it is released in advance, at that moment of time; as if the mainshock would share this energy with a foreshock, the accumulation process continuing up to the mainshock. In both cases, since $E \ll E_1$ and $\tau \ll t_1$, we can obtain a relation between these two quantities by differentiating equation (2),

$$\tau/t_0 = r(E_1/E_0)^{r-1}(E/E_0) \tag{3}$$

By using the definition of the magnitude, $E/E_0 = e^{bM}$, where $b = 3.45$ (3/2 in decimal logarithms) is the well-known Hanks-Kanamori constant (equation (B3)), this equation reads

$$\tau = \tau_0 e^{bM} \tag{4}$$

where

$$\tau_0 = r t_0 e^{-b(1-r)M_0} \tag{5}$$

is a small threshold time which depends on the magnitude of the mainshock (M_0) and the parameter of the background seismic activity (t_0 and r, $\beta = br$, see Appendix B). The small threshold time τ_0 indicates a very short quiescence time [Ogata and Tsuruoka, 2016] before (and after) the occurrence of the main shock ($\tau > \tau_0$). In addition, the time τ should be cut off by an upper threshold, at least for M not to be greater than the magnitude M_0 of the main shock ($M < M_0, \tau < \tau_0 e^{bM_0}$). The law given by equation (4) is valid in the proximity of a mainshock for relatively small times and magnitudes.

We note that the parameters of the background seismicity for Vrancea region, as discussed above, are $-\ln t_0 = 11.32$ (t_0 measured in years) and $\beta = 2.26$, such that, from $r = \beta/b$, where $b = 3.45$ (Appendix B), we get $r = 2.26/3.45 = 0.65$. These parameters are used in equation (5) for applications to Vrancea region.

Equation (4) can also be written as

$$M = \frac{1}{b} ln(\tau/\tau_0) \tag{6}$$

This equation tells that the magnitude M of a foreshock, or aftershock, is related to the time τ left until the mainshock, or elapsed after the mainshock, by a formula which depends on the parameters of the mainshock (M_0 in τ_0, equation (5)) and the parameters of the background seismicity. This dependence means that the foreshocks and the aftershocks are correlated to the mainshock. These are time-magnitude correlations [Apostol, 2021], which may also be called energy-energy correlations, since they involve an energy sharing. Together with the meaning of the differentiation given above, we may view these correlations as a description of the "physical" processes involved in the sequence foreshocks-mainshock-aftershocks. Basically, the mainshock shares its energy with the foreshocks and the aftershocks. However, specific features related to the stress accumulation or transfer, and the spatial distributions of these processes remain unknown.

4. Methods and results

Equation (6) can also be written as

$$M(t) = \frac{1}{b} \ln \frac{t_{ms} - t}{\tau_0} \tag{7}$$

where t_{ms} is the occurrence time of the mainshock. This equation can be fitted to the foreshock magnitudes for the parameters t_{ms} and τ_0 ($b = 3.45$). From τ_0 and equation (3), by making use of the parameters of the background seismicity (t_0, β, r), we can get the magnitude M_0 of the mainshock. Equation (4) is limited by $t_{ms} - t > \tau_0$ and a higher cutoff which accounts for $M < M_0$ at least ($t_{ms} - t < \tau_0 e^{bM_0}$).

It is worth noting that the time t_{ms} depends on the magnitude of the mainshock, as expected. For instance, a magnitude M indicates a time $\tau = \tau_0 e^{bM}$ up to the mainshock. Let us assume that we are interested in a mainshock with magnitude $M_0 = 7$; then by using $t_0 = e^{-11.32}$ (years, for Vrancea) and $r = 0.65$ given above, we get $\tau_0 = \frac{2}{3} 10^{-8.42}$ (years);

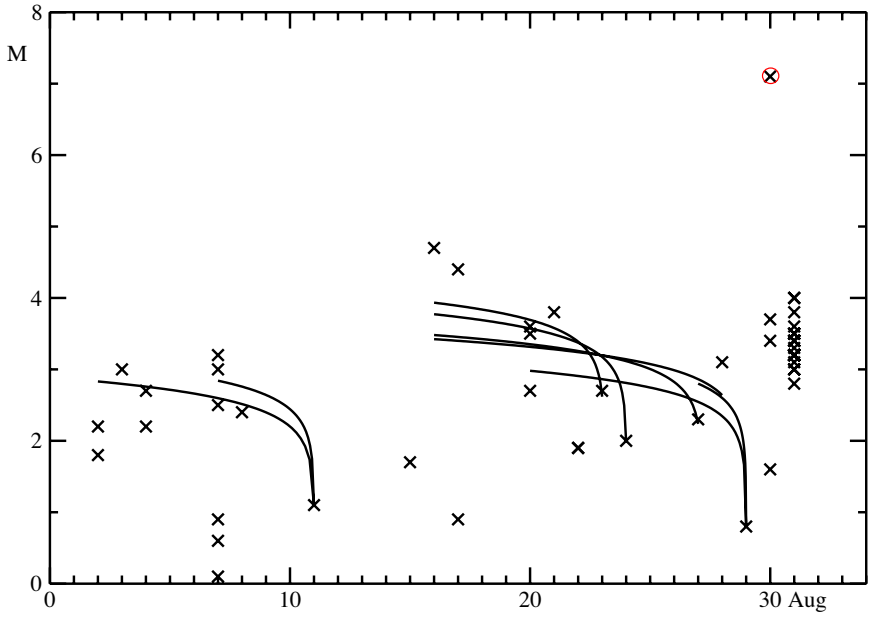

Figure 1. Vrancea seismic activity in the period 1 August-31 August 1986 [Romanian Earthquake Catalog, 2023], with several fitting curves of foreshock sequences. The fit of equation (7) to data from 16 August to 24 August gives the fitting parameters t_{ms} = 24 August and $\tau_0 = 10^{-4.76}$ days. This indicate that we are in the proximity of a mainshock.

a correlated foreshock with magnitude $M = 5$ would indicate that we are at $\tau = \frac{2}{3}10^{-8.42} \cdot 10^{7.5} = 0.079$ years, i.e. $\simeq 29$ days, from that mainshock.

We note that equation (7) has a very high slope in the neighbourhood of t_{ms}, such that a reliable estimation of the fitting parameters t_{ms} and τ_0 can only be achieved by a special data set, which would include, ideally, many small-magnitude foreshocks with magnitudes falling rapidly to zero. The importance of the small-magnitude foreshocks in assessing the foreshock-mainshock occurrence mechanism has been emphasized by Mignan [2014]. This would imply a small τ_0, which is difficult to attain. Consequently, we expect a systematic under-estimation of the mainshock magnitude M_0 (small τ_0 involves large M_0, according to equation (5).

Vrancea is the main seismic region of Romania. Three strong earthquakes occurred in Vrancea, since we have reliable recordings: magnitude $M = 7.1$, 30 August 1986; magnitude $M = 6.9$, 30 May 1990; magnitude $M = 6.4$, 31 May 1990 [Romanian Earthquake Catalog, 2023, http://www.infp.ro/data/romplus.txt]. We have applied the fitting procedure described above to the 7.1-earthquake of 30 August 1986 (depth 131 km). This earthquake and all its precursory events since 1 August are shown in Fig. 1. All these earthquakes occurred in an area with dimensions $\simeq 100$ km $\times$ 80 km (45°-46° latitude, 26°-27° longitude), at various depths in the range 30 km-170 km, except for the events of 7-8 August and the 1.6-event of 30 August, whose depths was 5 km-20 km. As shown in Fig. 1, we can identify several magnitude-descending sequences, which we fitted by equation (7). For earthquakes which occurred in the same day we have used the maximum magnitude (an average magnitude for the days with multiple events leads to a fit with larger errors). The fitting parameters are given in Table 1. We note large fitting errors, and a systematic under-estimation of the mainshock magnitude.

A particular example is the foreshock sequence from 16 August to 24 August (seven earthquakes), whose fitting parameters are t_{ms}=24 August, $\tau_0 = 10^{-4.76}$ days and a large *rms* relative error 0.32. These fitting parameters indicate the occurrence of a mainshock with magnitude 4.4 on 24 August. The data of the foreshocks in the sequence 16-24 August are given in Table 2. We can see that the hypocentres of these foreshocks are placed in an area with dimensions $\simeq 25$ km $\times$ 40 km, at depths in the range $\simeq 50$ km, centered on $\simeq 125$ km, except for one (24 August) placed at depth $\simeq 75$ km.

Another example is the sequence 7-11 August (four earthquakes), which includes surface foreshocks with closely neighbouring hypocentres and depths in the range 20-50 km.

We cannot identify magnitude-descending sequences for the earthquake pair of 30-31 May 1990 (depth 87-91 km). This is an example of a false negative of the method.

1986	t_{ms}	M_0	τ_0 (days)	*rms* relative error
2-11 August	11.02 August	1.37	$10^{-3.21}$ days	0.13
7-11	11	2.26	$10^{-3.66}$	0.11
16-23	23.07	5.03	$10^{-5.08}$	0.33
16-24	24	4.4	$10^{-4.76}$	0.32
16-27	27.15	3.31	$10^{-4.17}$	0.35
16-28	29.07	2.9	$10^{-4.00}$	0.35
20-29	29	1.96	$10^{-3.51}$	0.27
27-29	29	2.72	$10^{-3.90}$	0.16

Table 1. Various foreshock sequences for the $M = 7.1$ Vrancea mainshock, 30 August 1986, fitted by equations (7) and (5).

1986	Lat (°)	Long (°)	Depth (km)	*M*
16 August	45.58	26.33	148	4.7
17	45.74	26.38	44.5	0.9
17	45.67	26.47	104.8	4.4
20	45.55	26.37	165	2.7
20	45.53	26.57	122.3	3.6
20	45.64	26.67	143.2	3.5
21	45.66	26.54	146.7	3.8
22	45.60	26.70	102	1.9
22	45.62	26.11	31.8	1.9
23	45.69	26.57	140.5	2.7
24	45.75	26.18	74.6	2

Table 2. The foreshock sequence from 16 August to 24 August 1986, with the position of their hypocentres. For foreshocks occurring in the same day the maximum magnitude has been used for fitting.

The same procedure has been applied to the Vrancea earthquake with magnitude 3.8 (local magnitude 4.1), viewed as a mainshock, which occurred on 30 November 2021, where we used the foreshock sequence from 24 November to 29 November (six earthquakes). We estimate a mainshock with magnitude 4.5 on 1 December ([Apostol and Cune, 2021]; the data are taken from Romanian Earthquake Catalog, 2023, http://www.infp.ro/data/romplus.txt). All these foreshocks occurred within 45.47°-45.73° latitude, 26.26°-26.59° longitude, at depths in the range 90 km-130 km.

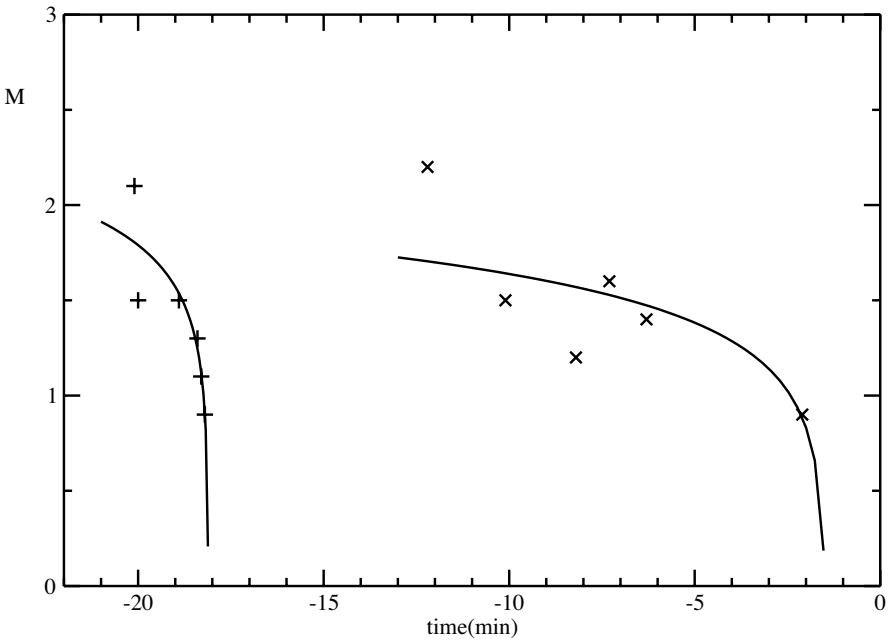

Figure 2. Two foreshock sequences, a few minutes before the Izmit earthquake, 17 August 1999, $M = 7.6$ fitted by the time-magnitude correlation equation (7).

We have analyzed the set of precursory events of the l'Aquila earthquake, 6 April 2009 (moment magnitude 6.3, local magnitude 5.9), where we identified two magnitude-descending sequences, with earthquakes succeeding rapidly at intervals of hours. The first sequence, consisting of seven earthquakes with local magnitudes from 2.1 to 1.0, occurred on 2 April. The fitting of these data indicates a mainshock approximately 5 hours before the earthquake with magnitude 3.0 of 3 April (with a large *rms* relative error 0.4). The second sequence consists of five earthquakes with magnitudes from 1.9 to 1.1, which occurred on 6 April. The fit, with a similar large error, indicates the occurrence of a mainshock at the time 01:35; the l'Aquila earthquake occurred at 01:32 (UTC; the last foreshock was recorded at 01:20). The data used in this analysis are taken from the Bollettino Sismico Italiano, 2002-2012 (https://www.earth-prints.org/handle/2122/10183) [2015], in $\pm$ 25 km an area around the epicenter of the l'Aquila earthquake (42.342° latitude, 13.380° longitude). The lack of the background seismicity parameters β and $-\ln t_0$ prevents us from estimating the magnitude of the mainshocks for l'Aquila. We note that the use of local magnitudes in equation (7) generates (small) errors.

For the Yangbi (Yunnan, China) earthquake of 21 May 2021, 13.48 hours, with (surface-wave) magnitude $M_s = 6.4$, depth $\simeq$ 5 km, we have identified two magnitude-decreasing sequences of foreshocks, each set located in a small spatial region, with an average depth $\simeq$ 5 km ([Zhu et al., 2022], Supplemental Materials, Table S1). The fitting of the first sequence of 19 May, from 12.06 hours, $M_s = 4.5$, to 16.54 hours, $M_s = 2.8$ (four earthquakes), predicts a mainshock on 19 May, 16.9 hours. The second set of foreshocks, on 21 May, from 13/21 hours/minutes, $M_s = 5.3$, to 13/40, $M_s = 2.8$ (three earthquakes), gives a mainshock on 21 May, 13.66. In both cases the parameter τ_0 is very small (abrupt decrease in magnitude), with an accelerating seismicity rate in the proximity of the mainshock. The fits have a small *rms* relative error 0.06 and 0.14. (Using equation (7) with the moment magnitude M replaced by the magnitude M_s introduces small errors).

A similar analysis has been performed for the Izmit (Turkey) earthquake of 17 August 1999, magnitude $M = 7.6$, depth 15 km ([Ellsworth and Bulut, 2018], Supplementary Information, Table 1). We have analyzed two foreshock

Earthquake: region, date, time of occurrence, magnitude	Foreshocks sequences: date, time, magnitude	Predicted time of occurrence
Yangbi, 21 May 2021, 13.48, M_S=6.4	19 May: hours 12.06, M_S=4.5; hours 12.28, M_S=2.9; hours 13.13, M_S=3.8; hours 16.54, M_S=2.8	t_{ms}=16.9 (hours)
Yangbi, 21 May 2021, 13.48, M_S=6.4	21 May: hours/minutes 3/21, M_S=5.3; hours/minutes 13/37, M_S=3.4; hours/minutes 13/40, M_S=2.8	t_{ms}=13.66 (hours)
Izmit, 17 August 1999, 00:01.44, M=7.6	16 August; time before (minutes): 20.1, M=2.1; 20, M=1.5; 18.9, M=1.5; 18.4, M=1.3; 18.3, M=1.1; 18.2, M=0.9	t_{ms}=18 (minutes before)
Izmit, 17 August 1999, 00:01.44, M=7.6	16 August; time before (minutes): 12.2, M=2.2; 10.1, M=1.5; 8.2, M=1.2; 7.3, M=1.6; 6.3, M=1.4; 2.1, M=0.9	t_{ms}=1.47 (minutes before)

Table 3. Foreshock time-magnitude sequences for the Yangbi earthquake ([Zhu et al., 2022], Supplemental Materials, Table S1), and the Izmit earthquake ([Ellsworth and Bulut, 2018], Supplementary Information, Table 1), and the predicted time of occurrence of the mainshock.

sequences, occurred on 16 August 1999, very close to the hypocentre of the mainshock, from minute 20.1 ($M = 2.1$) to 18.2 ($M = 0.9$) before the mainshock and from minute 12.2 ($M = 2.2$) to 2.1 ($M = 0.9$). These sequences predict a mainshock to the minute 18 and the minute 1.47 in advance, with a relatively low seismicity rate (slowly decreasing in magnitude) and small *rms* relative error 0.1 and 0.16. The fitting curves to the two Izmit sequences are shown in Fig. 2.

The data of the foreshock sequences used for the Yangbi earthquake and the Izmit earthquake are given in Table 3.

5. Discussion and conclusions

5.1 Forecasting

We have presented above a procedure which can be used in short-term forecasting of seismic mainshocks. The procedure is based on the correlations which may be present between foreshocks and the mainshock. The presence of the correlations has a random character. It is not necessary that they exist always, and we do not know apriori when they exist or not. According to the theory, these correlations produce an abrupt magnitude-descending sequence of foreshocks in the proximity of a mainshock; we should note that not all magnitude-descending precursory events are necessarily correlated foreshocks. Prior to a mainshock (as well as in the subsequent lapse of time) the local seismic conditions of the focal region may suffer changes, which are unknown. The theoretical considerations on which the present procedure is based assume that all the factors which may intervene remain the same. In particular, one component of the procedure – the determination of the magnitude of the mainshock – assumes that the background seismicity preserves its statistical parameters. Consequently, the procedure presented above may exhibit important limitations. For instance, between the moment of forecasting and the predicted occurrence moment of a mainshock the local seismic conditions may change, or the magnitude-decreasing foreshock sequence is not correlated, such that we may have a false positive. Similarly, a mainshock may be preceded by uncorrelated foreshocks, which may lead to a false negative. Nevertheless, if correlations are present and nothing else changes, we can forecast the occurrence time and even the magnitude of a mainshock, by using the abrupt magnitude-decreasing sequence of

correlated foreshocks which occur in its both spatial and temporal proximity. In some cases these conditions are fulfilled, in some other cases they are not. We cannot say apriori which case is which.

5.2 Time variation of the Gutenberg-Richter parameter

Closely related to the time-magnitude correlations described above is the so-called time variation of the Gutenberg-Richter β parameter. Let us compare equation (4) ($\tau = \tau_0 e^{bM}$) with equation (B4) given in Appendix B ($t = t_0 e^{\beta M}$). Equation (B4) gives the accumulation time for an independent (background, regular) earthquake with magnitude M. Accordingly, equation (4) may be viewed as giving the accumulation time for an independent earthquake with magnitude M, in different seismicity conditions, because the parameters τ_0 and b in this equation are different from the parameters t_0 and β in the former equation. Obviously, this interpretation applies to aftershocks, which may be viewed as independent earthquakes accumulating energy, in different seismicity conditions, following the mainshock. Indeed, it is reasonable to assume that after a mainshock the local seismicity conditions of the focal region are changed, and the corresponding parameters t_0 and β are changed into τ_0 and b. Although the law given by equation (4) holds for foreshocks too, such an interpretation does not hold for foreshocks, because the foreshocks occur in advance of the process of accumulating energy in time τ, also, probably, as a result of changes in the local structure of the region. It follows that the Gutenberg-Richter parameter β (GR parameter) is changed for aftershocks into the parameter $b > \beta$.

The corresponding Gutenberg-Richter magnitude distribution $(t_0/t^2)dt = \beta e^{-\beta M} dM$, which follows from the accumulation law (see Appendix B), is changed for aftershocks into $(\tau_0/\tau^2)d\tau = be^{-bM} dM$, which indicates an increase in the GR parameter ($b = 3.45$) with respect to its background value β (e.g., 2.3). We may assume that such a deviation is relevant up to a cutoff magnitude M_c where the two distributions become equal, such that we may estimate an average increase in the parameter β as $(b - \beta)/2\beta = 25\%$ for $\beta = 2.3$. The cutoff magnitude is given by $be^{-bM_c} = \beta e^{-\beta M_c}$, hence $M_c = 0.36$ for $r = 2/3$, $b = 3.45$ ($\beta = 2.3$). This estimation is in quantitative agreement with data reported by Gulia and Wiemer [2019] for the Amatrice-Norcia earthquakes (24 August 2016, magnitude 6.2; 30 October 2016, magnitude 6.6) and the Kumamoto earthquakes (15 April 2016, magnitude 6.5 and 7.3). These authors found that the aftershock parameter is higher than the background value (e.g., by 25%), while the foreshock parameter β is lower than the background value (e.g., by 10%). Also, a similar decrease in the parameter β has been reported for the foreshocks of the L'Aquila earthquake (6 April 2009, magnitude 6.3) by Gulia et al. [2016] and the Colfiorito, Umbria-Marche, earthquake (26 September 1997, magnitude 6) by De Santis et al. [2011].

In some cases, the aftershocks dominate the seismic activity subsequent to a mainshock. In those cases, a determination from empirical data of an increase in the GR parameter of the aftershocks can be achieved by a statistical analysis, providing we have a sufficiently large number of (statistically homogeneous) aftershocks. In some cases such a situation may not be present, in the sense that we may not have a sufficiently large number of events, or other factors, like the background seismic activity, may interfere. Such particularities in the statistical analysis of the foreshocks and the aftershocks have been pointed out by Dascher-Cousineau et al. [2020, 2021] (see also Gulia and Wiemer [2021]).

We turn now to another type of correlations, which may be relevant in the variability of the GR parameter of the accompanying events. Besides sharing energy with the mainshocks, we may view the accompanying seismic events as sharing also their accumulation time with the mainshocks. In this case the statistical analysis should reflect the time-time correlations, described in Appendix C.

As shown in Appendix C, the correlation-modified magnitude distribution (modified GR distribution, [Apostol, 2021]) is

$$P^c(M) = \beta e^{-\beta M} \frac{2}{(1 + e^{-\beta M})^2} \tag{8}$$

(equation (C3)); without other specifications, this distribution includes the time-time (or purely dynamical) correlations, which affect mainly the small-magnitude earthquakes. From equation (8) we get the correlation-modified cumulative distribution

$$P^c_{ex}(M) = e^{-\beta M} \frac{2}{1 + e^{-\beta M}} \tag{9}$$

The logarithmic form of this distribution

$$\ln N^c(M) = \ln N(0) + \ln 2 - \ln\left(1 + e^{\beta M}\right) \tag{10}$$

should be compared to the standard logarithmic form

$$\ln N(M) = \ln N(0) - \beta M \tag{11}$$

(equation (1)). We can see that the modified GR distributions (equations (8) and (9)) differ from the standard GR distributions. It seems that such a qualitative difference has been found for southern California earthquakes recorded between 1945-1985 and 1986-1992 [Jones, 1994]. The difference arises mainly in the small-magnitude region $M \simeq 1$, where the distribution is flattened. For instance, in this region the parameter β of the cumulative distribution tends to $\beta/2$, according to equations (8) and (9) (see Appendix C). This deviation, known as the roll-off effect [Bhattacharya et al., 2009; Pelletier, 2000], is assigned usually to an insufficient determination of the small-magnitude data. We can see that it may be due to correlations, at least partially. For large magnitudes the logarithmic cumulative distribution is shifted upwards by $\ln 2$ (equation (10)), while its slope is very close to the slope of the standard cumulative GR distribution (β).

The distribution given by equation (9) indicates a change in the parameter β of the standard GR distribution. We denote by B the modified parameter β; it is given by

$$e^{-\beta M}\frac{2}{1+e^{-\beta M}} = e^{-BM} \tag{12}$$

where B is a function of M ($B(M)$). It is convenient to introduce the ratio $R = B/b$ (similar to $r = \beta/b$ given above). We may view the earthquake with magnitude M as an earthquake which shares energy with a mainshock of magnitude M_0,

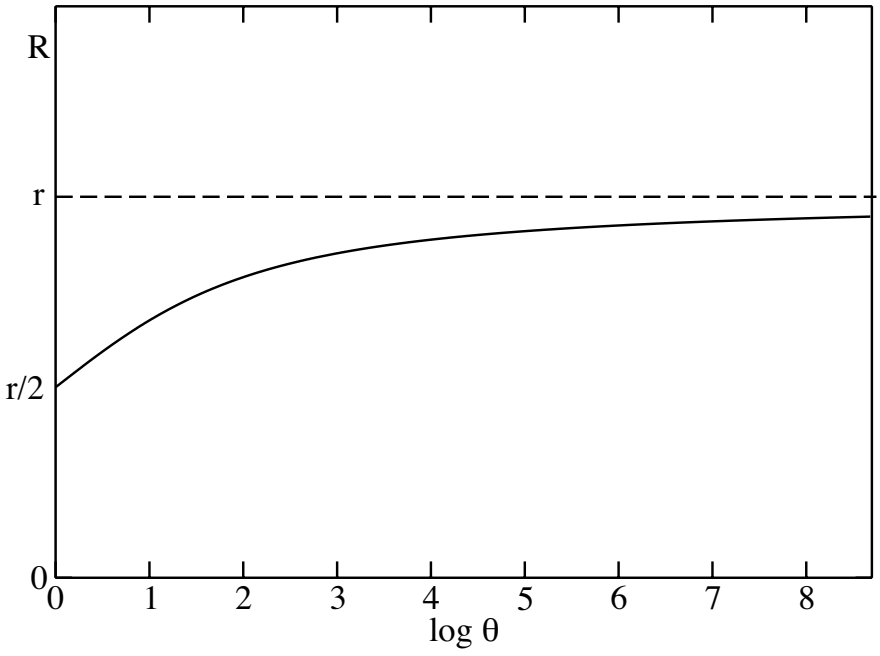

Figure 3. Function $R(\theta)$ vs $\log\theta$ for $r = 2/3$ (equation (13)).

such that we may use equation (6) for $e^{bM} = \tau/\tau_0$. Equation (12) becomes

$$R = \frac{1}{\ln\theta}\ln\left[\frac{1}{2}(1+\theta^r)\right] \tag{13}$$

where $\theta = {}^{\tau}/_{\tau_0}$. The use of equation (6) in equation (12) is valid in the proximity of a mainshock, where both time-magnitude and time-time correlations are present. The parameter R varies form $R = r$ for large values of the variable θ to $R = r/2$ for $\theta \to 1$ ($\tau \to \tau_0$). The function $R(\theta)$ is plotted in Fig. 3 *vs* $\log\theta$ for $r = 2/3$.The decrease of the function $R(\theta)$ for $\theta \to 1$ indicates correlations.

According to equation (12), the modified GR parameter B is given approximately by

$$B(M) \cong \beta - \frac{\ln 2}{M} \tag{14}$$

or

$$R(\tau) \cong r - \frac{\ln 2}{\ln({}^{\tau}/_{\tau_0})} \tag{15}$$

for a reasonable range of magnitudes $M > 1$. Equations (13)-(15) show the decrease of the GR parameter, as seen in some cases in a foreshock sequence. For instance, a 10% decrease is achieved for $M = 3$, or $\tau/\tau_0 \simeq 3.6 \times 10^4$ ($\beta = 2.3$, $r = 2/3$). This estimation is in quantitative agreement with data reported by Gulia and Wiemer [2019]. It is worth noting that smaller magnitudes occur in the sequence of correlated foreshocks for shorter times, measured from the occurrence of the mainshock (the nearer mainshock, the smaller correlated foreshocks). The determination of such a variation of the parameter β from empirical data can be attained in statistically valid conditions, when both time-magnitude and time-time correlations are present.

Acknowledgements. The authors are indebted to the colleagues in the Institute of Earth's Physics, Magurele-Bucharest, for many enlightening discussions. The authors are also indebted to the anonymous Reviewers for very useful comments, questions and suggestions. This work was carried out within the Program Nucleu SOL4RISC, contract no. 24N/03.01.2023, project no. PN23360202/2023 and Program Nucleu, contract no. 21N/09.01.2023, project no. PN23210101/2023 funded by the Romanian Ministry of Research, Innovation and Digitization. Data used for the Vrancea region have been extracted from the Romanian Earthquake Catalog, 2023, http://www.infp.ro/data/romplus.txt, 10.7014/SA/RO. Data used for l'Aquila earthquake (6 April 2009) are taken from the Bollettino Sismico Italiano, 2002-2012 (https://www.earth-prints.org/handle/2122/10183) [2015].

References

Apostol, B.F. (2006). A model of seismic focus and related statistical distributions of earthquakes, Phys. Lett. A357, 462-466, doi: 10.1016/j.physleta.2006.04.080.

Apostol, B.F. (2019). An inverse problem in seismology: derivation of the seismic source parameters from *P* and *S* seismic waves, J. Seismol. 23, 1017-1030.

Apostol, B.F. (2021). Correlations and Bath's law, Results in Geophysical Sciences 5, 100011.

Apostol, B.F. and L.C. Cune (2021). Prediction of Vrancea Earthquake of November 30, 2021, Seism. Bull. 2, Internal Report National Institute for Earth Physics, Magurele.

Bhattacharya, P., C.K. Chakrabarti and K.D. Kamal and Samanta (2009). Fractal models of earthquake dynamics, In Reviews of Nolinear Dynamics and Complexity, 107-150, Schuster, H. H., ed., NY, Wiley.

Bollettino Sismico Italiano, 2002-2012 (2015). http://bolettinosismica.rm.ingv.it., https://www.earth-prints.org/handle/2122/10183.

Bouchon, M., H. Karabulut, M. Aktar and S. Ozalaybey (2011). Extended nucleation of the 1999 M_w 7.6 Izmit earthquake, Science 331, 877-880.

Bouchon, M., V. Durand, D. Marsan, H. Karabulut and J. Schmittbuhl (2013). The long precursory phase of most large interplate earthquakes, Nature Geoscience, 6, 299-302, doi:10.1038/ngeo1770.

Dascher-Cousineau, K., T. Lay and E.E. Brodsky (2020). Two foreshock sequences post Gulia and Wiemer (2019), Seism. Res. Lett. 91, 2843-2850.

Dascher-Cousineau, K., T. Lay and E.E. Brodsky (2021). Reply to "Comment on 'Two foreshock sequences post Gulia and Wiemer (2019)' by K. Dascher-Cousineau, T. Lay, and E. E. Brodsky" by L. Gulia and S. Wiemer, Seism. Res. Lett. 92, 3259-3264.

De Santis, A., G. Cianchini, P. Favali, L. Beranzoli and E. Boschi (2011). The Gutenberg-Richter law and entropy of earthquakes: two case studies in Central Italy, Bull. Sesim. Soc. Am., 101, 1386-1395.

Ellsworth, W.L. and G.C. Beroza (1995). Seismic evidence for an earthquake nucleation phase, Science, 268, 851-855.

Ellsworth, W. and F. Bulut (2018). Nucleation of the 1999 Izmit earthquake by a triggered cascade of foreshocks, Nature Geoscience, 11, 531-535, https://doi.org/10.1038/s41561-018-0145-1.

Enescu, B., Z. Struzik and K. Kiyono (2008). On the recurrence time of earthquakes: insight from Vrancea (Romania) intermediate-depth events, Geophys. J. Int., 172, 395-404 and References therein.

Felzer, K.R., R.E. Abercrombie and G.A. Ekstrom (2004). Common origin for aftershocks, foreshocks and multiplets, Bull. Sesim. Soc. Am., 94, 88-98.

Frohlich, C. and S.D. Davis (1993). Teleseismic b values; or much ado about 1.0, J. Geophys. Res., 98, 631-644.

Gerstenberg, M.C., S. Wiemer, L.M. Jones and P.A. Reasenberg (2005). Real-time forecasts of tomorrow's earthquake in California, Nature, 435, 328-331.

Gulia, L., T. Tormann, S. Wiemer, M. Herrmann and S. Seif (2016). Short-term probabilistic earthquake risk assessment considering time-dependent b values, Geophys. Res. Lett., 43, 1100-1108.

Gulia, L., A.P. Rinaldi, T. Tormann, G. Vannucci, B. Enescu and S. Wiemer (2018). The effect of a mainshock on the size distribution of the aftershocks, Geophys. Res. Lett., 45, 13277-13287.

Gulia, L. and S. Wiemer (2019). Real-time discrimination of earthquake foreshocks and aftershocks, Nature, 574, 193-199.

Gulia, L. and S. Wiemer (2021). Comment on "Two foreshock sequences post Gulia and Wiemer (2019)" by K. Dascher-Cousineau, T. Lay, and E. E. Brodky, Seism. Res. Lett., 92, 3251-3258.

Helmstetter, A. and D. Sornette (2003). Foreshocks explained by cascades of triggered seismicity, J. Geophys. Res.: Solid Earth 108, https://doi.org/10.1029/2003JB002409.

Jones, L.M. and P. Molnar (1976). Frequency of foreshocks, Nature, 262, 677-679.

Jones, L.M. and P. Molnar (1979). Some characteristics of foreshocks and their possible relationship to earthquake prediction and premonitory slip of faults, J. Geophys. Res., 84, 3596-3608.

Jones, L.M. (1994). Foreshocks, aftershocks and earthquake probabilities: accounting for the Landers earthquake, Bull. Seism. Soc. Am., 84, 892-899.

Jordan, T.H., Y. Chen, P. Gasparini and R. Madariaga (2011). Operational earthquake forecasting: state of knowledge and guidelines for utilization, Ann. Geophys. 54, 315-391.

Lay, T. and T.C. Wallace (1995). Modern Global Seismology, Academic Press, San Diego, California.

Lippiello, E., F. Giacco, W. Marzocchi, C. Godano and L. de Arcangelis (2015). Mechanical origin of aftershocks, Sci. Reps., 15560, doi:10.1038/srep15560.

Mignan, A. (2011). Retrospective on the accelerating seismic release (ASR) hypothesis: Controversy and new horizons, Tectonophysics, 505, 1-16.

Mignan, A. (2014). The debate on the prognostic value of earthquake foreshocks: A meta-analysis, Sci. Reps., 4099, doi:10.1038/srep04099.

Ogata, Y. (1998a). Statistical models for earthquakes occurrences and residual analysis for point processes, J. Amer. Statist. Assoc., 83, 9-27.

Ogata, Y. (1998b). Space-time point-process models for earthquakes occurrences", Ann. Inst. Statist. Math., 50, 379-402.

Ogata, Y. and H. Tsuruoka (2016). Statistical monitoring of aftershock sequences: a case study of the 2015 M_w 7.8 Gorkha, Nepal, earthquake, Earth, Planets and Space, 68, 44, 10.1186/s40623-016-0410-8.

Ohnaka, M. (1992). Earthquake source nucleation: A physical model for short-term precursors, Tectonophysics, 211, 149-178.

Omori, F. (1894). On the aftershocks of earthquakes, J. College of Science, Imp. Univ. Tokyo, 7, 111-200.

Papazachos, B.C. (1975). Foreshocks and earthquake predictions, Tectonophysics, 28, 213-226.

Pelletier, J.D. (2000). Spring-block models of seismicity: review and analysis of a structurally heterogeneous model coupled to the viscous asthenosphere, in Geocomplexity and the Physics of Earthquakes, 120, Rundle, J.B., D.L. Turcotte and W. Klein, eds. NY, Am. Geophys. Union.

Petrillo, G. and E. Lippiello (2020). Testing of the foreshock hypothesis within an epidemic like description of seismicity, Geophys. J. Int., 225, 1236-1257.

Romanian Earthquake Catalog (2023). http://www.infp.ro/data/romplus.txt, 10.7014/SA/RO.

Saichev, A. and D. Sornette (2005). Vere-Jones' self-similar branching model, Phys. Rev., E72, 056122.

Seif, S., J.D. Zechar, A. Mignan, S. Nandan and S. Wiemer (2019). Foreshocks and their potential deviation from general seismicity, Bull. Seism. Soc. Am., 1-18, doi: 10.1785/0120170188.

Stein, S. and M. Wysession (2003). An Introduction to Seismology, Earthquakes, and Earth Structure, Blackwell, NY.

Udias, A. (1999). Principles of Seismology, Cambridge University Press, NY.

Utsu, T. (1965). Aftershocks and earthquake statistics, J. Fac. Sci. Hokkaido Univ. Ser. VII 3, 379441.

van Stiphout, T., S. Wiemer and W. Marzocchi (2010). Are short-term evacuations warranted? Case of the 2009 l'Aquila earthquake, Geophys. Res. Lett., 37, L06306.

Yamashita, F., E. Fukuyama, S. Xu, H. Kawakata, K. Mizoguchi and S. Takizawa (2021). Two end-member earthquake preparations illuminated bu foreshock activity on a meter-scale laboratory fault, Nature Commun., 12, 4302, doi: 10.1038/s41467-021-24625-4.

Zhu, G., H. Yang, Y.J. Tan, M. Jin, X. Li and W. Yang (2022). The cascading foreshock sequence of the $M_s = 6.4$ Yangbi earthquake in Yunnan, China, Earth and Planet. Sci. Letts., 591, 117594.

***CORRESPONDING AUTHOR: Bogdan FELIX APOSTOL**,
National Institute for Earth Physics, Călugăreni Street, 12 Magurele, Ilfov, Romania
e-mail: afelix@theory.nipne.ro

ANNALS OF GEOPHYSICS, 66, 6, 2023; doi:10.4401/ag-8964

APPENDIX TO

ON THE RELEVANCE OF THE FORESHOCKS IN FORECASTING SEISMIC MAINSHOCKS

Bogdan Felix Apostol[1] and Liviu Cristian Cune[2]

[1] National Institute for Earth Physics, Călugăreni Street, 12 Magurele, Ilfov, Romania
[2] National Institute of Physics and Nuclear Engineering, Magurele, Ilfov, Romania, MG-6, POBox MG-35, Romania

1. A: Geometric-growth model of energy accumulation in focus

In Apostol [2006] a typical earthquake is considered, with a small focal region localized in the solid crust of the Earth. The dimension of the focal region is so small in comparison to our distance scale, that we may approximate the focal region by a point in an elastic body. The movement of the tectonic plates may lead to energy accumulation in this point-like focus. The energy accumulation in the focus is governed by the continuity equation (energy conservation)

$$\frac{\partial E}{\partial t} = -\boldsymbol{v} grad E \tag{A1}$$

where E is the energy, t denotes the time and $\boldsymbol{v}$ is an accumulation velocity. For such a localized focus we may replace the derivatives in equation (A1) by ratios of small, finite differences. For instance, we replace $\partial E/\partial x$ by $\Delta E/\Delta x$ for the coordinate x, etc. Moreover, we assume that the energy tends to zero at the borders of the focus, such that $\Delta E = -E$, where E is the energy in the centre of the focus. Also, we assume a uniform variation of the coordinates of the borders of this small focal region, given by equations of the type $\Delta x = u_x t$, where $\boldsymbol{u}$ is a small displacement velocity of the medium in the focal region. The energy accumulated in the focus is gathered from the outer region of the focus, as expected. With these assumptions equation (A1) becomes

$$\frac{\partial E}{\partial t} = \left(\frac{v_x}{u_x} + \frac{v_y}{u_y} + \frac{v_z}{u_z}\right)\frac{E}{t} \tag{A2}$$

Let us assume an isotropic motion without energy loss; then, the two velocities are equal, $\boldsymbol{v} = \boldsymbol{u}$, and the bracket in equation (A2) acquires the value 3. In the opposite limit, we assume a one-dimensional motion. In this case the bracket in equation (A2) is equal to unity. A similar analysis holds for a two dimensional accumulation process. In general, we may write equation (A2) as

$$\frac{\partial E}{\partial t} = \frac{1E}{rt} \tag{A3}$$

where r is an empirical (statistical) parameter; we expect it to vary approximately in the range (1/3,1). We note that equation (A3) is a non-linear relationship between t and E. The parameter r may give an insight into the geometry of the

focal region. Also, it reflects the structural condition of the focal region, by the relation between the two velocities $\boldsymbol{v}$ and $\boldsymbol{u}$. We call this model a geometric-growth model of energy accumulation in the focal region.

It is shown in Appendix B that the parameter r is related to the Gutenberg-Richter parameter β and the Hanks-Kanamori constant $b = 3.45$ (3/2 in decimal logarithms) through $\beta = br$.

A special attention is given to shearing faults, which are typical earthquake sources. The energy accumulation takes place along one direction, say $u_x = v_x$, but the mass conservation requires, on the average, a motion in opposite directions along, say, the perpendicular y-axis [Apostol, 2019]. This makes $u_y = 2v_y$ (2 from the two opposite directions), which, together with $u_z = 0$, leads to $r = 2/3$. Indeed, this is the mean value of the ratio $r = \beta/b$, accepted as reference value ($\beta = 2.3$, $b = 3.45$, $r = 2/3$, see the main text).

The integration of equation (A3) needs a cutoff (threshold) energy and a cutoff (threshold) time. During a short time t_0 a small energy E_0 is accumulated. In the next short interval of time this energy may be lost, by a relaxation of the focal region. Consequently, such processes are always present in a focal region, although they may not lead to an energy accumulation in the focus. We call them fundamental processes (or fundamental earthquakes, or E_0-seismic events). It follows that we must include them in the accumulation process, such that we measure the energy from E_0 and the time from t_0. The integration of equation (A3) leads to the law of energy accumulation in the focus

$$t/t_0 = (E/E_0)^r \tag{A4}$$

The time t in this equation is the time needed for the accumulation of the energy E, which may be released in an earthquake (the accumulation time). This is the time-energy accumulation equation referred to in the main text.

2. B: Gutenberg-Richter law. Time probability

The well-known Hanks-Kanamori law reads

$$\ln \overline{M} = const + bM \tag{B1}$$

where $\overline{M}$ is the seismic moment, M is the moment magnitude and $b = 3.45$ (3/2 for base 10). In Apostol [2019] the relation $\overline{M} = 2\sqrt{2}E$ has been established, where $\overline{M} = \left(\Sigma_{ij} M_{ij}^2\right)^{1/2}$ (mean seismic moment), M_{ij} is the tensor of the seismic moment and E is the energy of the earthquake. If we identify the mean seismic moment with $\overline{M}$ we can write

$$\ln E = const + bM \tag{B2}$$

(another *const*), or

$$E/E_0 = e^{bM} \tag{B3}$$

where E_0 is a threshold energy (related to *const*). Making use of equation (A4), we get

$$t = t_0 e^{brM} = t_0 e^{\beta M} \tag{B4}$$

where $\beta = br$. From this equation we derive the useful relation $dt = \beta t_0 e^{\beta M} dM$, or $dt = \beta t dM$. If we assume that the earthquakes are distributed according to the well-known Gutenberg-Richter distribution,

$$dP = \beta e^{-\beta M} dM \tag{B5}$$

we get the distribution

$$dP = \beta \frac{t_0}{t} \frac{1}{\beta t} dt = \frac{t_0}{t_2} dt \tag{B6}$$

[Apostol, 2006]. This law shows that the probability for an earthquake to occur between t and $t + dt$ is $\frac{t_0}{t^2} dt$; since the accumulation time is t, the earthquake has an energy E and a magnitude M given by the above formulae (equations (B2) and (B3)). The law given by the equation (B5) is also derived [Apostol, 2021] from the definition of the probability of the fundamental E_0-seismic events ($dP = -\frac{\partial}{\partial t} \frac{t_0}{t} dt$). We note that this probability assumes independent earthquakes.

3. C: Time-time correlations

In general, if two earthquakes are mutually affected by various conditions, and such an influence is reflected in the above equations, we say that they are correlated to each other. Of course, multiple correlations may exist, *i.e.* correlations between three, four, etc. earthquakes. We limit ourselves to two-earthquake (pair) correlations. Very likely, correlated earthquakes occur in the same seismic region and in relatively short intervals of time. The physical causes of mutual influence of two earthquakes are various. In Apostol [2021] three types of earthquake correlations are identified. In one type the neighbouring focal regions may share energy. Since the energy accumulation law is non-linear, this energy sharing affects the occurrence time. We call these correlations time-magnitude correlations (or energy-energy correlations), as described in the main text. They are a particular type of dynamical correlations. In a second type of correlations, to be described below, two earthquakes may share their accumulation time, which affects their total energy. We call such correlations time-time, or purely dynamical correlations. Both these correlations affect the earthquake statistical distributions; in this respect, they are also statistical correlations. Finally, additional constraints on the statistical variables (*e.g.*, the magnitude of the accompanying seismic event be smaller than the magnitude of the main shock) give rise to purely statistical correlations.

Let us assume that an earthquake occurs in time t_1 and another earthquake follows in time t_2. The total time is $t = t_1 + t_2$, such that these earthquakes share their accumulation time, which affects their total energy. These are time-time (or purely dynamical) correlations. According to equation (5) (and the definition of the probability), the probability density of such an event can be obtained

$$-\frac{\partial}{\partial t_2} \frac{t_0}{(t_1 + t_2)^2} = \frac{2t_0}{(t_1 + t_2)^3} \tag{C1}$$

(where $t_0 < t_1 < +\infty, 0 < t_2 < +\infty$). By passing to magnitude distributions ($t_{1,2} = t_0 e^{\beta M_{1,2}}$), we get

$$d^2P = 4\beta^2 \frac{e^{\beta(M_1+M_2)}}{(e^{\beta M_1} + e^{\beta M_2})^3} dM_1 dM_2 \tag{C2}$$

(where $0 < M_{1,2} < +\infty$, corresponding to $t_0 < t_{1,2} < +\infty$, which introduces a factor 2 in equation (C1)). This formula (which is a pair, bivariate statistical distribution) is established in Apostol [2021]. (We note that there is no restriction upon M_2 in comparison with M_1, in contrast to the time-magnitude correlations). If we integrate equation (C2) with respect to M_2, we get the distribution of a correlated earthquake (marginal distribution)

$$dP = \beta e^{-\beta M_1} \frac{2}{(1 + e^{-\beta M_1})^2} dM_1 \tag{C3}$$

If we integrate further this distribution from $M_1 = M$ to $+\infty$, we get the correlated cumulative distribution

$$P(M) = \int_M^\infty dP = e^{-\beta M} \frac{2}{1 + e^{-\beta M}} \tag{C4}$$

From $M \gg 1$ the correlated distribution becomes $P(M) \simeq 2e^{-\beta M}$ and $\ln P(M) \simeq \ln 2 - \beta M$, which shows that the slope β of the logarithm of the independent cumulative distribution (Gutenberg-Richter, standard distribution $e^{-\beta M}$) is not changed (for large magnitudes); the correlated distribution is only shifted upwards by ln 2. On the contrary, for small magnitudes ($M \ll 1$) the slope of the correlated distribution becomes $\beta/2$ ($P(M) \simeq 1 - \frac{1}{2}\beta M + \cdots$ by a series expansion of equation (C4)), instead of the slope of the Gutenberg-Richter distribution ($e^{-\beta M} \simeq 1 - \beta M + \cdots$). The time-time correlations modify the slope of the Gutenberg-Richter standard distribution for small magnitudes. This is the roll-off effect referred to in the main text.